

€ 350: Nucl. Phys. B145, 45-66  
(1978)

N  
N 3145, 67 (78)

*Reprinted from:*

NUCLEAR PHYSICS

**INCLUSIVE  $\pi^0$  AND  $\eta$  PRODUCTION FROM 100 GeV/c  $\pi^+p$  COLLISIONS  
IN THE TRIPLE RIDGE REGION \***

A.V. BARNES, G.C. FOX \*\*, R.G. KENNEDY and R.L. WALKER  
*California Institute of Technology, Pasadena, California 91109*

O.I. DAHL, R.W. KENNEY, A. OGAWA and M. PRIPSTEIN  
*Lawrence Berkeley Laboratory, Berkeley, California 94720*



NORTH-HOLLAND PUBLISHING COMPANY - AMSTERDAM

## INCLUSIVE $\pi^0$ AND $\eta$ PRODUCTION FROM 100-GeV/c $\pi^0 p$ COLLISIONS IN THE TRIPLE REGGE REGION \*

A.V. BARNES, G.C. FOX \*\*, R.G. KENNEDY and R.L. WALKER  
*California Institute of Technology, Pasadena, California 91109*

O.I. DAHL, R.W. KUNNEY, A. OGAWA and M. PRIPSTHIN  
*Lawrence Berkeley Laboratory, Berkeley, California 94720*

Received 15 August 1978

Results are given for inclusive  $\pi^0$  and  $\eta$  production in 100-GeV/c  $\pi^0 p$  collisions. The data cover the large  $x \gtrsim 0.7$  region and are compared in detail with the predictions of triple Regge theory. These reactions are theoretically clean with  $\pi\eta\pi^0$  production or  $A_2(\eta)$  production exchange. We extract the Regge trajectories,  $\alpha(t)$ , in the  $t$  range of 0 to  $-4$  (GeV/c) $^2$ . We find good agreement with the determination from  $\pi^+ p \rightarrow (\pi^0, \eta) n$  at low  $-t$  while for large  $-t \gtrsim 1.3$  (GeV/c) $^2$ , the value of  $\alpha$  becomes approximately  $-0.3$ , independent of  $t$ . We see evidence for the wrong-signature nonet zero of the  $\rho$  at  $t = -0.4$  (GeV/c) $^2$  in the  $\pi^0$  production data. In agreement with simple Regge theory, there is no structure in the  $\eta$  production data at this  $t$  value.

### 1. Introduction

We present results on the inclusive reactions



where the detected  $\pi^0$  or  $\eta$  lies in the kinematic region  $0 \leq -t \leq 4$  (GeV/c) $^2$  and  $x \gtrsim 0.7$  and the incident  $\pi^+$  or  $\pi^0$  beam has a momentum of 100-GeV/c. These reactions may be described by the triple Regge model [1-3], which allows an interpretation of the data in terms of the  $\rho$  and  $A_2$  trajectories for the  $\pi^0$  and  $\eta$  respectively. The results are compared with those from experiment E811 at Fermilab, which used the same photon detector to measure the corresponding exclusive processes [4].



\* Work supported in part by the US Department of Energy under Contract No. EY76-C-03-0064 (Caltech) and Lawrence Berkeley Laboratory Contract No. N-7405-Eug-48.

\*\* Supported in part by the Alfred P. Sloan Foundation.

In our case, the  $x$  dependence gives the Regge trajectories whereas, for the exclusive processes, they are derived from the  $t$  dependence. Hence we have been able to obtain the trajectories from data taken at just one beam energy.

The reactions (2) provide the best tests of ordinary Regge theory because of their simplicity in the  $t$ -channel, i.e., only one trajectory is exchanged in each case. Likewise, (1) provides the best tests of triple Regge theory as again there is essentially only one triple Regge term present. As an additional bonus, the inclusive cross sections are several orders of magnitude higher than for the exclusive processes and so we have been able to measure these reactions out to higher  $-t$  than was possible with (2). The results of this paper and the accompanying one [8] on the all neutral final state  $\pi^0$  and  $\eta$  production provide striking evidence for the validity of triple Regge theory at low  $-t$ . Assuming that this interpretation remains valid at larger  $-t$ , we are able to extend our knowledge of the  $\rho$  and  $A_2$  trajectories out to  $t = -4$  (GeV/c) $^2$  and find that they become approximately independent of  $t$ . There have been many previous experiments [2,3,6] testing triple Regge theory but they have been mainly on diffractive reactions, such as  $p\bar{p} \rightarrow pX$ , where many triple Regge terms can contribute. Thus it has not been possible before to provide really clean tests of the theory. We believe that our data confirm and quantify the success of triple Regge theory suggested by the diffractive experiments.

In sect. 2, we describe the experimental setup and in sect. 3, we discuss the processing of the photon detector data. Both these sections may be omitted if desired. In sect. 4, we present the results and a discussion of their theoretical interpretation and we finish with our conclusions in sect. 5.

## 2. Apparatus and trigger

The data were taken in the M2 secondary beam at Fermilab using the apparatus shown schematically in fig. 1. The beam particle ( $\pi$ -K-p) was identified using two helium gas-filled differential Cherenkov counters, the first of which is omitted from the sketch. Since we shall discuss only incident pions in this paper, we applied very strict software cuts which gave negligible contamination from kaons and protons. The flux was corrected for the electron contamination which was determined from Cherenkov counter measurements. The direction of the beam particle was determined using two widely separated hodoscopes. Satisfactory beam particles were defined using electronics described in ref. [7]. The pion interacted in a 60 cm long liquid hydrogen target and the produced  $\pi^0$ 's and  $\eta$ 's were detected by their 2-photon decay mode. The photon detector, shown in the inset to fig. 1, was a 75 cm square hodoscope containing 21 radiation lengths of lead scintillator sandwich. The shower energy was integrated in the longitudinal direction by counters consisting of eight scintillation rods, each 1 cm wide, 0.7 cm thick, and 73.5 cm long, which were evenly spaced in depth and coupled to one phototube. There were

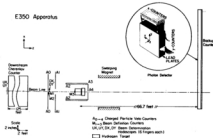


Fig. 1. Schematic arrangement of the experimental apparatus. The inset shows the photon detector in more detail.

Twenty such counters in each of two orthogonal directions so that the photon showers were seen in two transverse directions ( $x$  and  $y$ ). For this experiment, a "backup counter", consisting of about four radiation lengths of lead scintillator sandwich with ten counters in the  $x$  direction, was attached to the back of the main detector in order to sample the energy leaking out the back of the main detector and hence improve the energy resolution, as described in sect. 3. Since in this experiment we are looking for  $\pi^{\pm}$ 's produced in conjunction with charged particles, we desired to minimize the number of charged particles hitting the detector to help our event reconstruction. To do this, we used a sweeping magnet and placed the detector at such a distance that the magnet did not aperture interactions in the target. The magnet swept charged particles in the horizontal direction, so we placed the detector off-center (17 counter widths into the beam line) so that non-interacting beam particles just missed one edge. Two hodoscopes were used to determine the directions of the beam particles.

The data presented here were taken with two different triggers. The first required that the total energy deposited in the photon detector be above some threshold energy. The second required that the energy in a region of the detector away from the beamline corresponding to  $-t \gtrsim 1$  (GeV/c) $^2$  be above a threshold. Several threshold energies were used to provide a complete coverage of the kinematic region under consideration. The data from these triggers have been combined together in the results presented here. Two other triggers used in this experiment were the

Neutral Final State trigger, described in ref. [5], and one requiring an incident kaon or proton, which we shall present in a later paper.

### 3. Event analysis

We show a typical event in fig. 2. The data consist of twenty pulse heights in each of two orthogonal views ( $x$  and  $y$ ) and ten pulse heights from the backup counter in the  $x$  direction, which are not shown. We see that several showers are present. Our problem is to identify pairs of photons which come from the decay of  $\pi^0$  or  $\eta$ 's. For example, a  $\pi^0$  with an energy of 100 GeV decays into two photons which are separated by a minimum of 5 counter widths when they hit the detector. Photons from lower energy  $\pi^0$ 's have greater separation. Each photon then produces an electromagnetic shower whose transverse development has a FWHM of about 1 counter width. Hence the two showers are distinct in at least one view. However, they may not be separated from other photons present in the event. In our example, two  $\pi^0$ 's are present with photons  $\alpha$  and  $\beta$  belonging to the higher-energy one, in which we are interested, and photons  $\gamma$  and  $\delta$  to the other. In the  $x$  view, all the photons are distinct but in the  $y$  view, the photon showers from  $\beta$  and  $\delta$  have merged. Actually most events are simpler to analyze than that illustrated in fig. 2 for, as shown in table 1, three quarters of the events have only the two:

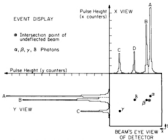


Fig. 2. A typical event. A, B, C and D indicate the observed peaks in each view and  $\alpha$ ,  $\beta$ ,  $\gamma$  and  $\delta$  the positions of the photons on the face of the detector.  $\alpha$  and  $\beta$  form the  $\pi^0$  in the triple Regge region.

Table 1  
Backgrounds under  $\pi^0$  and  $\eta$  peaks

Produced particle	Photons in detector	$ y  \leq 1.0$ (GeV/c) $^2$		$ y  \geq 1.0$ (GeV/c) $^2$	
		Fraction of events	Background/signal	Fraction of events	Background/signal
$0.37 < y < 0.68$					
$\pi^0$	2	0.75	0.008	0.71	0.005
	$> 2$	0.25	0.18	0.29	0.09
$\eta$	2	1.00	0.41	0.59	0.3
	$> 2$	0.00		0.41	6
$0.68 < y < 0.78$					
$\pi^0$	2	0.79	0.005	0.84	0.003
	$> 2$	0.21	0.14	0.16	0.06
$\eta$	2	1.00	0.24	0.79	0.3
	$> 2$	0.00		0.21	3
$0.78 < y < 0.86$					
$\pi^0$	2	0.87	0.004	0.81	0.004
	$> 2$	0.13	0.11	0.19	0.06
$\eta$	2	0.98	0.14	0.93	0.3
	$> 2$	0.02	10	0.07	4
$y > 0.86$					
$\pi^0$	2	0.95	0.002	0.96	0.002
	$> 2$	0.05	0.01	0.04	0.08
$\eta$	2	0.99	0.01	1.00	0.4
	$> 2$	0.01	10	0.00	

photons from the  $\pi^0$  or  $\eta$  decay in the detector. We developed software that both optimized the recognition of  $\pi^0$ 's and  $\eta$ 's in a multiphoton environment and improved the  $\pi^0$  and  $\eta$  energy resolution. The analysis was based on the fact that the transverse development of a shower is subject to only small statistical fluctuations. We use the observed shape of a pulse-height peak (A-D in fig. 2) both to tell if it consists of more than one photon whose showers have coalesced in one view and to improve our resolution.

The analysis involved three main steps:

- (a) determination of the response of the detector as a function of the energy and the transverse distance of a photon from the center of a counter,
  - (b) determination of the gain of the phototubes as a function of time,
  - (c) constrained fits to all information recorded for a given event.
- Let us describe these in order.

## (a) Shower shape

The response of the detector to photons was found iteratively. To a good approximation, the response of the detector was found to be linear in energy. The transverse shape,  $S(d, E)$ , i.e., the pulse height in a counter that was distance  $d$  in one view from a photon of energy  $E$ , was found by looking at a sample of single photons. Our knowledge of the  $d$  and  $E$  dependence of  $S$  was then refined by varying  $S$  about this first approximation to minimize the goodness of fits to  $\pi^0$ 's and  $\eta$ 's observed in a part of the data sample. This involved looking at about 100 000  $\pi^0$ 's and essentially meant that we minimized the  $\chi^2$  of the constrained fit described in (c) with respect to parameters defining  $S(d, E)$ . Details of the resultant function may be found elsewhere [8].

## (b) Photomultiplier gains

The time dependence of the gains was monitored throughout the experiment for each counter using  $^{229}\text{Po}$  sources in scintillator discs mounted between the logic light pipes and the photomultiplier cathodes. The absolute value of each gain was found in a manner similar to that used to determine  $S(d, E)$ , namely the gains of all 140 counters were varied to minimize the  $\chi^2$  of constrained fits averaged over very many  $\pi^0$ 's. This worked well but the imperfect knowledge of the gains is still an important contribution to our energy resolution (see (c) below). This was because the source monitoring system was not set up perfectly and there was some residual time dependence corresponding on average to about a 1% uncertainty in the gains.

## (c) Constrained fits

To make maximum use of the information available, the parameters of each event were determined by a  $\chi^2$  fit to the 140 observed pulse heights in the detector. For an event with  $n$  photons ( $n = 4$  in fig. 2), we have 3 $n$  parameters: an energy  $E_i$  and  $x$  and  $y$  intercepts  $x_i$  and  $y_i$  for the  $i$ th photon. The pulse heights can be predicted in terms of  $E_i$ ,  $x_i$  and  $y_i$ , using the shower shape function  $S(d, E)$  discussed in (a). The proper errors in  $S(d, E)$  were determined by the procedure used to find  $S$  itself and, using these, a weighted  $\chi^2$  was minimized.

The invariant mass of two photons of energies  $E_1$  and  $E_2$  and angular separation,  $\theta_{12h}$ , is given by,

$$m^2 = E_1 E_2 \theta_{12h}^2 \quad (2)$$

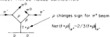
The angular separation  $\theta_{12h}$  was determined from the intercepts,  $x_i$  and  $y_i$ , of the photons on the detector assuming that the interaction was at the midpoint of the target. The energies of the photons were initially determined by the pulse heights and detector calibration. However, we used constrained fits where the energies were forced to satisfy (2) with  $m$  equal to the  $\pi^0$  or  $\eta$  mass. Interestingly enough, this gives a substantial improvement in the resolution for the energy  $E = E_1 + E_2$  of the  $\pi^0$  or  $\eta$ . In fact, for a 100 GeV  $\pi^0$ , the raw energy resolution of the detector, determined from  $E = E_1 + E_2$  using the pulse heights only and assuming that the gains are exactly known, is 2%. In a perfect world, use of (2) as described above

CONTRIBUTIONS TO  $\pi^0 p \rightarrow \pi^0 X$ 

## A. DOMINANT TRIPLE REGGE FORM

 $\pi^0$  beam =  $\pi^+$  beam

## B. SMALLI TRIPLE REGGE CORRECTION

Note that  $p_{\mu}^2 \approx 0.733 p_{\mu}^2$ .

## C. LOW MASS CONTRIBUTIONS

By Duality  
Total resonances  $[\rho] \rightarrow 2/3$  Total resonances.

## D. 1-2 CONTRIBUTIONS



1-2 pion

Fig. 4. Contributions to  $\pi^0 p \rightarrow \pi^0 X$  in the triple Regge region, discussed in text 4.

The exchange, shown in fig. 4b, with the pomeron replaced by the combination  $f = \sqrt{2}f_1 + \sqrt{3}f_2$  for  $\pi^0$  beams gives

$$\frac{d^2\sigma}{dx^2} \approx \frac{G_3^2(t)}{\sqrt{t}} (1 - \beta)^{0.3 - 2\alpha_M}, \quad (6)$$

where we have assumed that  $a_0(0) = a_2(0) = 0.5$  and also that  $G_3^2(t) = \frac{2}{3}G_2^2(t) \parallel 10$ . Actually, (6) is a very small contribution to the cross section and we are rather insensitive to it. We see this directly from our raw data which show that the cross sections from the  $\pi^+$  and  $\pi^-$  beams are about equal (see fig. 12b) as predicted by (5) and not  $\frac{2}{3}$  as given by (6). So we decided to fix its contribution using a theoretical estimate, as we shall see, varying this estimate by a factor of 2 making a negligible effect. One can estimate (6) from the analogous terms found in the  $p\bar{p} \rightarrow pX$  analysis of ref. [2]. This analysis used finite mass sum rules [11] (FMSR); one can try to use the FMSR directly on our data but our poor mass resolution makes this hard, although we did find results consistent with the  $p\bar{p} \rightarrow pX$  data. We have a large sample of data at an incident momentum of 200 GeV/c, when the analysis of this is complete, we may be able to pin down (6) from its beam-energy dependence.

At high  $x$ , we find contributions from the production of resonances of low mass,

$M \approx \sqrt{s}(1-x)$ , shown in fig. 4c. By duality, these are related to the  $\mu\bar{\mu} \pi^0\pi^0$  contribution discussed above. We have explicitly included the reactions

$$\pi^+ p \rightarrow \pi^0 n, \quad \pi^+ p \rightarrow \pi^0 \Delta^0, \quad \pi^+ p \rightarrow \pi^0 \Delta^+ \quad (7)$$

The cross sections for these processes were estimated using the ELL results [4] and our all neutral final state data [5]. Our data indicate that (7) underestimates the low-mass contribution, presumably the higher mass  $N^0$ 's and  $\Delta$ 's can also contribute significantly to the full inclusive reaction whilst giving little contribution to the all neutral final state due to the predominance of decays involving charged particles. We are not aware of any measurement of their (charge-exchange) cross section. The triple Regge terms were cut off at a missing mass above the  $\Delta$  mass and the data were fit only up to  $x = 0.98$ , i.e.,  $M = 2$  GeV, so it was not all sensitive to these low-mass terms. We have not subtracted the contribution of  $\pi^0$ 's and  $\eta$ 's from the decays of  $K^0$ 's,  $\omega$ 's,  $\eta'$ 's, etc.

The reactions  $\pi^+ p \rightarrow \pi^0 X$  allow meson  $J=1$  and  $J=2$  exchange in the  $\pi^+\pi^0$  channel. Normally, one would expect the  $J=2$  part to be negligible but it can be produced by  $\pi$  exchange, shown in fig. 4d, and turns out to be surprisingly large at small  $-t$ .  $J=2$  exchange is directly probed by the reactions  $\pi^+ p \rightarrow \pi^+ X$  or  $\pi^- p \rightarrow \pi^0 X$ . However, the only high  $x$  measurements have been of  $\pi^+ p \rightarrow \pi^- X$  at  $p_t = 0.3$  and 0.5 GeV/c and  $x \leq 0.9$  [12]. Hence we have used to calculate this term using a particular model based on  $\pi$  exchange. We suppose that two real pions are produced at the incident pion vertex and a virtual pion is exchanged so that the observed pion and the incident pion are in a state of isospin = 2. This vertex can then be calculated using known  $\pi\pi$  scattering amplitudes [13, 14].<sup>8</sup> The virtual pion and proton interaction is calculated using the np total cross section. With no free parameters present, this model gave good agreement with the  $\pi^+ p \rightarrow \pi^+ X$  data. This model was suggested in ref. [12] where it was calculated using  $\rho$  and  $f$  production as shown in fig. 4d. We prefer to use the full  $\pi\pi$  scattering amplitudes, this gives similar results to the calculations in ref. [12]. Note that resonances of higher mass than the  $f$ , e.g., the  $g$ , give small contributions because  $J=2$  exchange in  $\pi^+ p \rightarrow \pi^0 X$  is generated by  $J=2$  exchange in the  $\pi\pi$  amplitude. As  $J=2$  is an exotic exchange, it is expected to be small at high  $\pi\pi$  masses and experimentally this prediction seems to set in above the  $f$  [14]. We emphasize that we only expect the model to be reliable at small  $-t$  where one is reasonably insensitive to extrapolations off the  $\pi$  pole, thus we only use this correction below  $-t \sim 0.3$  (GeV/c)<sup>2</sup>. Fortunately, we only expect the term to be big at the small  $-t$  values where we can calculate it because only here do we get significant enhancement from the  $\pi$  pole. Finally, we note that explicit inclusion of the  $J=2$  term is not equivalent to just subtracting the  $\rho$ ,  $f$  resonance production contributions. In fact, the  $\rho$  and  $f$  contribute equally to  $J=1$  and 2 in the  $\pi^+\pi^0$  channel. We believe that the  $J=1$  part of  $\rho$ ,  $f$  production is

<sup>8</sup> Ref. [13] has a compilation of  $\pi\pi$  scattering amplitudes.

already "included" in the triple Regge term (5.6), certainly duality would suggest this [11].

The discussion of  $\eta$  production is completely analogous to the  $\pi^0$  case except that there is no  $J=2$  contribution and one must exchange the  $A_2$  instead of the  $\rho$  Regge pole.

#### 4.2. Tracing triple Regge theory: determination of the $\rho$ trajectory

We have binned the data in  $t$  bins and fitted the  $x$  dependence to the triple Regge terms (5.6), with the unknown parameters being the  $t$  dependent trajectory  $a_\rho(t)$  of the exchanged  $\rho$  and its  $\mu\text{GeV}$  residue,  $G_\rho(t)$ , defined by (5). We have

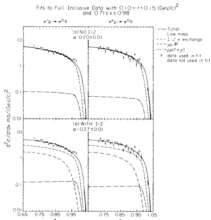


Fig. 3. Data on  $\pi^0 p \rightarrow \pi^0 X$  as a function of  $x$  for  $0.10 < -t < 0.15$ . The results of a fit to the  $\pi^0$  and  $\eta^0$  data simultaneously allowing  $a_\rho(t)$  and  $G_\rho(t)$  to vary are shown for (bottom)  $J=2$  term included and (top)  $J=2$  term included.

smeared the theoretical functions with the energy resolution and beam momentum distribution but have ignored the  $t$  resolution which is small compared with the size of the bins [8]. We have fitted the  $\pi^+$  and  $\pi^-$  data simultaneously, allowing  $a_\mu(t)$  and  $C_\mu(t)$  to vary. Data and fits for some representative  $t$  bins are shown in figs. 5–7 while the trajectories and residue functions derived from these fits are shown in fig. 8. Without looking in detail at the fits, we see from figs. 5–7 that the  $x$  dependence of the cross section changes dramatically with  $-t$ , at low  $-t$  it is roughly flat but at higher  $-t$  it falls rapidly with increasing  $x$ . This is, of course, predicted by triple Regge theory (5) from the change with  $t$  of  $a_0$  from  $\sim 0.4$  at  $t = 0$  to  $\sim 0.3$  at higher  $-t$ . This change in  $x$  dependence in the inclusive process is analogous to the famous shrinkage of  $\pi^+ p \rightarrow \pi^0 n$  [4].

In figs. 5–8, we show fits for the bins  $0.10 < -t < 0.15$  ( $\text{GeV}/c)^2$  and  $0.30 < -t < 0.40$  ( $\text{GeV}/c)^2$  with and without our parameterization of the  $J = 2$  contribution as already discussed. We have fixed the residue function of the  $p\bar{p}(f + p)$  term and used the same  $a_0$  as in the  $p\bar{p}P$  term. The figures show it to be a small contri-

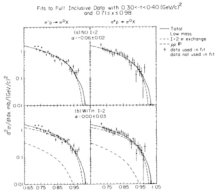


Fig. 6. Data on  $\pi^0 p \rightarrow \pi^0 X$  as a function of  $x$  for  $0.30 < -t < 0.40$ . The results of a fit are shown for (a) no  $J = 2$  term included and (b)  $J = 2$  term included.

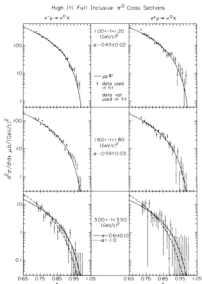


Fig. 7. Data on  $\pi^0 p \rightarrow \pi^0 X$  as a function of  $x$  for selected  $t$  bins at high  $-t$ . The curves are fits to the  $\mu_P$  term of triple Regge theory as described in the text, and the fitted values of  $\alpha$  and  $G$  are plotted against  $t$  in fig. 8.

bution. We see that the  $J=2$  term contributes about a quarter of the cross section and that its behavior is very different from a power of  $(1-x)$ . As expected, the importance of the  $J=2$  term is decreasing with increasing  $-t$ . Including the  $J=2$

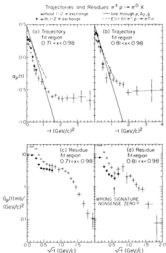


Fig. 8. The trajectory,  $\alpha_p(t)$ , and the residue function,  $G_p(t)$  determined from fits to the  $\mu\bar{\mu}$  and  $\rho\bar{\rho}$  terms using the  $\pi^0 p \rightarrow \pi^0 K$  data, for fits over  $0.71 < x < 0.98$  in (a) and (c) and fits over  $0.81 < x < 0.98$  in (b) and (d). Also shown is the parameterization of a trajectory from the exclusive  $\pi^- p \rightarrow \pi^0 n$  data [4] and the linear trajectory passing through the  $\pi$ ,  $A_2$  and  $\rho$

term raises the extracted value of  $\alpha_p(t)$  by about 0.1, as shown in figs. 8a,b, and leads to better agreement with the trajectory found from  $\pi^- p \rightarrow \pi^0 n$ . We also see that the trajectory obtained from the region  $0.81 < x < 0.98$  is in better agreement with the  $\pi^- p \rightarrow \pi^0 n$  value at low  $-t$  than that from the region  $0.71 < x < 0.98$ . Curiously there is still significant disagreement with  $\pi^- p \rightarrow \pi^0 n$  in fig. 8b for the

lowest  $t$  bin. At low  $-t$ , we always find that the data for high  $x \geq 0.97$  lie above our fits, presumably this is due to low-mass  $N^0$ 's (fig. 4c) not included in the fit.

We have investigated the sensitivity of the low  $-t$  results to our  $\rho\pi\Gamma + \rho\Gamma$  parameterization. We find that doubling or halving  $G(\rho)$  makes  $a_\mu$  decrease or increase by about 0.01 for  $-t \leq 0.25 \text{ (GeV/c)}^2$ . We have tested the sensitivity of the results to our knowledge of the beam momentum and the resolution. Increasing the beam momentum by 1% causes a decrease of  $a$  from 0.01 at low  $-t$  to 0.05 at high  $-t$ . Increasing the standard deviation of the resolution from 1.6% to 2.0% causes a change of less than 0.01 in  $a$ .

A sample of the high  $-t$  data is shown in fig. 7, where it is fitted to the  $\rho\pi\Gamma$  term only for  $0.71 \leq x \leq 0.98$ . We see from here and from fig. 8 that the trajectory flattens off at about  $-0.6$ . The uncertainty in this asymptote can be estimated by fitting in the region  $0.81 \leq x \leq 0.98$  which changes it up by 0.1 to  $a_\mu = -0.5$  as shown in fig. 8b.  $a_\mu = -0.5$  implies that the cross section behaves like  $(1-x)^2$ , the constituent interchange model [15] (CIM) predicts a leveling off of  $a_\mu$  at  $-1$  in a  $(1-x)^0$  cross-section behavior. The fit given by fixing  $a$  at  $-1$  and allowing just the normalization to vary is shown in fig. 7 for the  $0.00 \leq x \leq 0.50 \text{ (GeV/c)}^2$  bin.

Since triple Regge theory is only expected to be valid at high  $x$ , we see that our data suggest that the theory is indeed valid for  $x \geq 0.8$  but there are other sources of  $\pi^0$ 's present at lower  $x$ . At  $x = 0.7$ , we estimate they are 20% of the triple Regge term. The presence of such terms is also shown in fig. 5 where the fits lie below the lowest  $x$  data.

The residue function,  $G_\mu(t)$ , from the fit to the  $\rho\pi\Gamma$  term, is shown in figs. 8a-d. We see that there is a significant difference between whether the  $J=2$  term is included or not. But we see that, in both cases, it falls rapidly with  $-t$  for  $-t \leq 0.3 \text{ (GeV/c)}^2$ , and then has a change in slope. In (d), where the fit was over the restricted range  $0.81 \leq x \leq 0.98$ , we see a dip at  $t \approx -0.4 \text{ (GeV/c)}^2$  which is coincident with the place where the trajectory passes through zero. This is presumably the  $\rho$  wrong-signature nonsense zero seen more clearly in our neutral final state data [5]. The fact that from the fits for  $x > 0.81$ , we see both a  $\rho$  trajectory near the  $\pi^+ \pi^- \pi^0 n$  value and the  $\rho$  wrong-signature nonsense zero, suggests again that this is the region of validity of triple Regge theory.

#### 4.3. $\eta$ production

We also took data on the reaction  $\pi^0 p \rightarrow \eta N$  where the  $\eta$  decayed into two photons. We have corrected our data using a  $2\gamma$  branching ratio of 0.38. In the triple Regge model, these reactions are dominated by  $A_2 A_2 \Gamma^*$  exchange and have contributions at low  $-t$  from the  $A_3 A_2 (\Gamma^* \rho)$  and the low-mass resonance terms. We note that the  $\eta$  production should be a clearer test of triple Regge theory because it has no complications from  $J=2$  exchanges as the  $\eta$  is an isoscalar and also is less likely to be produced from the decay of another particle or have contributions from central production that could well be present for  $\pi^0$ 's.

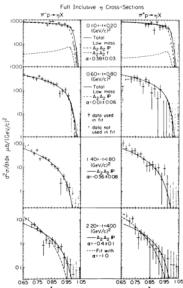


Fig. 9. Data on  $\pi^0 p \rightarrow \pi X$  as a function of  $x$  for selected  $t$  bins. The curves are fits to the  $A_2A_2P$  and  $A_2A_2F$  terms of triple Regge theory. The trajectory and residue functions from their fits are shown in fig. 10.

We fitted the  $\pi^+$  and  $\pi^-$  data simultaneously to find the  $A_2$  trajectory,  $\alpha_{A_2}(t)$ , and the residue function,  $G_{A_2}(t)$ . Selected cross sections are shown in fig. 9. For  $-t > 0.2 (\text{GeV}/c)^2$ , we fitted the data over  $0.71 < x < 0.98$  whilst for  $-t < 0.2$

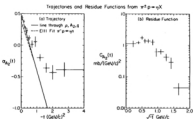


Fig. 10. Trajectory,  $a_{A_2}(t)$ , and residue function,  $G_{A_2}(t)$ , determined from fits to the  $A_2 A_2 \eta' p$  and  $A_2 A_2 \eta p$  terms using the  $\pi^0 p \rightarrow \eta X$  data. Also shown are the parameterization of the  $A_2$  trajectory from the exclusive  $\pi^0 p \rightarrow \eta n$  data [4] and the linear trajectory passing through the  $\rho$ ,  $A_2$  and  $\eta$ .

(GeV/c) $^2$  we fitted over  $0.81 < x < 0.98$  because the  $t_{\min}$  effect depletes the lower  $x$  region [8]. We see in fig. 9 how the  $x$  dependence of the data varies with  $t$ . Fig. 10 shows the resulting  $A_2$  trajectory and residue function. At low  $-t$ , the trajectory lies about 0.1 higher than the E8II result obtained from the exclusive reaction  $\pi^0 p \rightarrow \eta n$  [4] and about 0.2 higher than our  $\rho$  trajectory. It agrees well with the straight line through the  $\rho$ ,  $A_2$  and  $\eta$  at low  $-t$  and then curves away above it. Just as for  $\pi^0$  production, we see that the trajectory levels off at a value near -0.5. Comparing fig. 10b with 8d, we see that the  $A_2$  residue is completely featureless (and might even peak) at the  $t$  value where the  $\rho$  residue has its dip. This is a striking success for naive Regge theory.

#### 4.4. Cross sections

The cross sections for  $\pi^0 p \rightarrow \pi^0 X$  integrated over  $x$  from 0.71 to 0.81, from 0.81 to 0.91 and above 0.91 are shown in fig. 11. Here  $x$  is the detected  $\pi^0$  energy divided by the beam energy. We see that in all these energy bins, there is a change in slope at  $t = -0.45$  (GeV/c) $^2$ . Near this point,  $a_\rho(t)$  passes through zero and it is also where we see a "wrong signature nonsense zero" in our fits for  $x > 0.81$  and in our neutral final state data. Here we see only a break of slope (also a feature of the NPS data) but no dip. We show a fit of the integrated cross section for  $-t > -1.5$  (GeV/c) $^2$  to the form  $Ae^{Bt}$  where the normalization  $A$  is varied for the different  $x$  bins but where the parameter  $B$  is kept constant. The best fit gives  $B = 1.82$  (GeV/c) $^{-2}$  and we see that the data fit this form reasonably well.

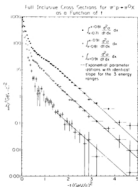


Fig. 11. The cross section  $\sigma^2 \rho/\text{mb}$  integrated over  $x$  between (a) 0.71 and 0.81, (b) 0.81 and 0.91 and (c) above 0.91 for the reaction  $p\bar{p} \rightarrow \pi^0 X$ . Here  $x = \text{detected } \pi^0 \text{ energy/beam energy}$ .

The ratio of the  $\eta$  cross section to the  $\pi^0$  cross section integrated over  $x > 0.71$  is shown in fig. 12a. The peak in the ratio at  $t \approx -0.5$  corresponds, of course, to the structure at this point shown in figs. 8c,d. The ratio at higher  $t$  flattens off to somewhere between 0.3 and 0.4. This is a little lower than the prediction of 0.5 made by assuming the simple argument that only the  $u\bar{u}$  and  $d\bar{d}$  content of the  $\pi^0$  and  $\eta$  is important and that  $\eta = \sqrt{\frac{1}{3}}(u\bar{u} - d\bar{d})$ . This prediction assumes that the  $u\bar{u}$  and  $d\bar{d}$  terms contribute incoherently. This is rather dangerous because in naive Regge theory (which we have found works at low  $-t$ ), the  $u\bar{u}$  and  $d\bar{d}$  parts of  $\eta$  interfere destructively at  $t \approx -1.5 \text{ (GeV/c)}^2$  where the  $A_2$  has its wrong signature nonsense zero. The incoherence assumption is justified in quark-quark scattering models for high  $p_\perp$  processes as described in ref. [16]. In the CIM model, we know of no estimates of  $\eta/\pi^0$  production; one would naively estimate zero as  $a_\rho = a_{A_2} = -1$  is predicted at high  $-t$  and here a simple Regge  $A_2$  contribution must vanish from the cancellation between  $u\bar{u}$  and  $d\bar{d}$  described above. Our  $\eta/\pi^0$  ratio is comparable to the value of  $0.44 \pm 0.05$  obtained at low  $x$  and high  $p_\perp$  using the same photon detector [17].

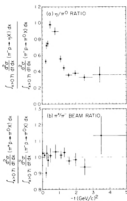


Fig. 12. The ratios of the integrated cross section,  $\int_{x_0}^{\infty} dx (d^2\sigma/dxdt)/dx$  for (a) ( $\pi^+ p \rightarrow \eta K^0$  or  $\pi^- p \rightarrow \pi^0 K^0$ ) and (b) ( $\pi^+ p \rightarrow \pi^0 K^0$  or  $\pi^- p \rightarrow \pi^0 K^0$ ).

The ratio of the  $\pi^+$  to  $\pi^-$  beam production of  $\pi^0$ 's is shown in fig. 12b. We see that the ratio is near 1 everywhere. This is in agreement with the dominance of the  $p\bar{p}P$  term. At the high  $-t$  values, one would predict the observed value of unity from either quark-quark scattering [16] or the constituent-interchange model [15], the latter would predict differences between  $\pi^+$  and  $\pi^-$  beams at higher  $-t$  values than those probed sensitively by this experiment.

### 5. Conclusions

We have found striking agreement between triple Regge theory for both the trajectory and residue functions of the  $\rho$  and  $A_2$ . The theory seems to be valid for  $x > 0.8$  although even here one must add the contribution of an  $J = 2$  exchange term for the  $\pi^0$  production. We have not investigated the importance of Regge cuts in our reactions even though we know from two-body scattering that they

must be present [18,19]. The dip in  $\pi^+ p \rightarrow \pi^0 n$  is popularly explained either as a pole-cut interference [19] or as the wrong-signature nonresonant zero of the  $\rho$  Regge pole. Only the latter model would naturally predict the dip at about the same  $t$  value that we see in our full inclusive data. Confirming the Regge explanation is the complete lack of any structure in our  $\eta$  data, as seen in fact in  $\pi^+ p \rightarrow \eta n$  [4], and the similar dip systematics in our all neutral data [5]. Actually, it may be possible to understand the dip in the  $\rho$  residue,  $G_\rho(t)$ , shown in fig. 8d, from just analyticity. Thus we can separate out the signature factor and write,

$$\begin{aligned} G_\rho(t) &\approx G'_\rho(t) \frac{(1 - e^{-im_\rho t})^2}{\sin^2 m_\rho t} = \\ &= G'_\rho(t)/\cos^2(\tfrac{1}{2}m_\rho t). \end{aligned} \quad (8)$$

Even if  $G'_\rho(t)$  has no structure at  $m_\rho = 0$ , we shall get a dip from the inverse cosine in (8) at  $m_\rho = 0$ . This could well explain the structure in both our neutral final state and full inclusive  $\rho$  residues. The dip in (8) comes from the signature factor which can be regarded as a necessary consequence of analyticity and the obtained  $(1 - x)^{1 - 2m_\rho t}$  behavior of the cross section. In simple Regge theory,  $G_\rho(t)$  is zero at  $m_\rho = 0$  as a consequence of  $\rho$ - $A_2$  exchange degeneracy. In this explanation of our data, the complete zero at  $m_\rho = 0$  in the cross section is filled in with other contributions.

Our trajectory functions level off at  $t \approx -0.5$  for  $-t \gtrsim 1.5 \text{ (GeV/c)}^2$  and we see this same universal behavior in our neutral final state data [5]. Is this to be attributed to the behavior of the  $\rho$  and  $A_2$  exchanges or is it some hard scattering contribution [15,16] swamping the Regge contributions? In the CIM model, the trajectories level off so that the Regge exchanges are the hard-scattering terms. It is not clear that this is true in all models. Experimentally, it could be understood by measuring  $a_0$  from  $\pi^+ p \rightarrow \pi^0 n$  at large  $-t$ .

In the CIM model, the high  $x$ , high  $-t$ , region probed by our data is understood in terms of the incident  $\pi^0$  scattering off a quark inside the proton, a typical process for  $\pi^+ p \rightarrow \pi^0 N$  would be  $\pi^+ u \rightarrow \pi^0 d$  where the initial  $u$  is in the sea of the proton and the final  $d$  fragments into a jet of hadrons. As pointed out before, this predicts  $a_0 \approx -1$  at high  $-t$ , which is somewhat lower than our observed value of  $-0.5$ . It is possible, of course, that the trajectory will reach  $-1$  at larger  $-t$  values than those probed in our experiment. Further, the exact value of  $a$  is sensitive to that definition of  $x$  used in the basic formula (5). We have used  $x$  as the lab energy divided by the maximum possible energy at the given  $t$  value, changing the definition so that the denominator is just the beam energy would decrease the fitted  $a$  by about 0.2 at  $-t = 4 \text{ (GeV/c)}^2$ . However, one can also estimate [20] the absolute value of the CIM term and for  $t \sim -3 \text{ (GeV/c)}^2$ , one finds a prediction that is about a factor of thirty below our data. So both the magnitude and energy dependence of our data suggest that the CIM model is not applicable to our high  $-t$  measurements.

Quark-quark and quark-gluon scattering is a fashionable model for high  $p_t$  processes near  $x = 0$  [16, 21]. Naturally, this will also contribute to the high- $x$  region. In this model, rather than the coherent process  $\pi^- n \rightarrow \pi^0 d$  of the CSM model, one has the incoherent processes typified by  $u_1 u_2 \rightarrow \bar{u}_3 u_4$  where the final  $u_3$  fragments into the observed  $\pi^0$ .  $u_1$  is a constituent of the  $\pi^-$  and  $u_2$  of the proton. Suppose the  $u$  and  $d$  distributions inside the  $\pi^-$  behave as  $(1 - x_q)^{\alpha_q}$  at  $x_q$ , the fraction of  $\pi^-$  momentum carried by the  $u$ ,  $d$  quarks,  $\rightarrow 1$ . Again suppose the fragmentation functions of quarks into  $\pi^0$ 's behave as  $(1 - z)^{\beta_{\pi^0}}$ , as  $z$ , the fraction of the quark ( $\bar{u}_3$  in example) momentum carried by the  $\pi^0$ ,  $\rightarrow 1$ . Then the apparent value of  $\alpha$  seen in our  $\pi^- p \rightarrow \pi^0 X$  data is predicted to be

$$\alpha_{QCD} = \alpha_q - 1 - \frac{1}{2}(n_1 + n_2),$$

where the basic quark-quark scattering has "Regge" intercept  $\alpha_q$ . In the QCD formulation of quark-quark scattering,  $\alpha_q = 1$  as it is single gluon (a spin-1 particle) exchange. Thus we get

$$\alpha_{QCD} = -\frac{1}{2}(n_1 + n_2).$$

Fashionable choices for  $n_1$ ,  $n_2$ , vary from  $n_1 = n_2 = 0$  (ref. [16]) to  $n_1 = n_2 = 1$  from the counting rules (ref. [22]). It is, therefore, quite possible that QCD can explain our observations. We need to know more about the  $\pi$  structure functions in order to be able to make reliable calculations.

Finally, one must mention the quark-recombination model [23,24] which has been applied to meson production from a proton beam at high  $x$  [25,26]. This is normally applied at low  $p_t$ , but clearly our data show that this region is dominated by triple Regge terms. Maybe it can provide a description of our high- $-t$  data where  $\alpha$  has settled down to its "universal" value of -0.5 but the corresponding  $(1 - x)^2$  behavior of the cross section at fixed  $t$  does not seem to be predicted by the model. The recent  $pp \rightarrow (\pi, K)X$  data from the CHLM collaboration show reasonable agreement with triple Regge theory for  $x > 0.7$  [27]. It seems likely that in this  $x$  region, at least, triple Regge theory and not quark recombination is the correct description of both of our pion and the CHLM proton induced reactions.

In conclusion, we see that the theoretical interpretation of our results is still unclear. The most economical explanation is a combination of triple Regge theory at low- $-t$  and hard scattering (QCD) at high- $-t$ . Any theoretical description should explain why we see such similar behavior in the all neutral and full inclusive data.

We should like to thank Joel Melkma and Alvin Tolleson for their invaluable help at the start of this experiment. Randy Johnson, Bruce Carter, Dave Henneyer and Aileen Stone were very helpful in the analysis and running of the experiment.

We acknowledge Rick Field's help and advice on the theoretical interpretation of our results. Geoffrey Fox thanks Hanna Miettinen for a discussion on the quark recombination model. Rosemary Kennett thanks the Fannie and John Hertz Foundation for Fellowship support.

## References

- [1] A.H. Mueller, Phys. Rev. D2 (1970) 2963, D4 (1971) 150.
- [2] R.D. Field and G.C. Fox, Nucl. Phys. B80 (1974) 367.
- [3] J. Butler, in BNL report no. BNL-30598, ed. H. Gordon and B.T. Pouch, Proc. Am. Phys. Soc. Meeting, Division of particles and fields, Upton, New York, 1976, unpublished.
- [4] A.V. Barnes et al., Phys. Rev. Lett. 37 (1976) 76.
- [5] O.B. Dahl et al., Phys. Rev. Lett. 37 (1976) 88.
- [6] A.V. Barnes et al., Nucl. Phys. B145 (1978) 47.
- [7] M.G. Albergo et al., Nucl. Phys. B108 (1976) 1.
- [8] R.A. Johnson, thesis, Lawrence Berkeley Laboratory report no. LBL-4610, 1973, unpublished.
- [9] R.C. Bennett, Caltech Ph.D. thesis, in preparation.
- [10] R.L. Walker, Attenuation of light in long oscillators, CALT-68-348 unpublished internal report (1972).
- [11] A.C. Irving, Roger results, Liverpool University preprint (1978).
- [12] M. Fukugita and K. Igi, Phys. Reports 31 (1977) 237.
- [13] D. Curré et al., Phys. Rev. Lett. 40 (1978) 141.
- [14] D. Nonneman, Nucl. Phys. B137 (1978) 443.
- [15] B. Hyams et al., Nucl. Phys. B164 (1973) 134.
- [16] D. Sivers, S. Brodsky and R. Blankenbecler, Phys. Reports 23 (1976) 1.
- [17] R.D. Field and R.F. Feynman, Phys. Rev. D15 (1977) 2290.
- [18] G.J. Donaldson et al., Phys. Rev. Lett. 40 (1978) 684.
- [19] A.C. Irving and R.F. Wودden, Phys. Reports 14 (1977) 117.
- [20] G.L. Kane and A. Scott, Rev. Mod. Phys. 48 (1976) 309.
- [21] R. Blankenbecler, S.J. Brodsky and J.L. Gunion, The magnitude of large transverse momentum cross sections, SLAC-PUB-2057 preprint (1977), Phys. Rev. D, to be published.
- [22] R.F. Feynman, R.D. Field and G.C. Fox, A quantum chromodynamic approach for the large transverse momentum production of particles and jets, CALT-68-431 preprint (1978).
- [23] S. Brodsky and G. Paus, Phys. Rev. D11 (1975) 1309.
- [24] W. Ochs, Nucl. Phys. B118 (1977) 397.
- [25] R.F. Dye and R. Hwa, Phys. Lett. 68B (1977) 409.
- [26] F.C. Iand and J.C. Sures, Parton interpretation of low  $p_T$  deep inelastic pp collisions at  $s = 2000$  GeV $^2$ , CERN preprint (1978).
- [27] J.R. Johnson et al., Phys. Rev. Lett. 39 (1977) 1173.
- [28] J. Singh et al., Nucl. Phys. B140 (1978) 189.

PRINTED IN THE NETHERLANDS